To experimentally determine that TE does indeed become zero for perfectly aligned crystals would be extremely difficult. This experiment would require that the crystals be aligned to within a tenth or even a hundredth of a degree since the crystals used in this work, which were aligned to within one degree, produced TE voltages as large as 10% of the magnetoresistance voltage. In addition, these crystals would have aligned in the magnetic field with the same accuracy.

The experimental evidence that TE is large for crystals misaligned by only one degree makes it difficult to believe that TE will not be observed when there is complete alignment. However, the very general nature of the crystal symmetry arguments almost forces one to assume that TE will be zero for perfectly aligned crystals.

APPENDIX B: VALUE OF PARAMETERS USED IN THE OPW CONSTRUCTION

Lattice constants for gallium at 4.2°K[19]:

$$a_0 = 4.5103\ \text{Å},$$
$$b_0 = 4.4861\ \text{Å},$$
$$c_0 = 7.6463\ \text{Å}.$$

Valence of gallium: 3.
Bravais lattice: base-centered orthorhombic.
Number of atoms per base-centered cell: 4.

[19] C. S. Barrett (private communication).

PHYSICAL REVIEW VOLUME 126, NUMBER 4 MAY 15, 1962

Symmetry and Free Electron Properties of the Gallium Energy Bands*

J. C. SLATER, G. F. KOSTER, AND J. H. WOOD
Department of Physics, Massachusetts Institute of Technology, Cambridge, Massachusetts
(Received December 18, 1961)

Atomic arrangement, unit cell, and Brillouin zone of metallic gallium are described, including notations for the various symmetry directions. The point and space groups are discussed, including character tables, and basis functions in the form of symmetrized plane waves for electronic wave functions of each symmetry type. The free-electron approximation is used as a first step toward finding the energy bands and Fermi surfaces. This work is preparatory toward a study of energy bands which is under way using the augmented-plane-wave method.

1. CRYSTAL STRUCTURE AND BRILLOUIN ZONE OF GALLIUM

A GREAT deal of experimental activity is going on at present with the aim of studying the Fermi surface of gallium.[1] We do not have a suitable theoretical treatment of the gallium energy bands. Consequently, we are preparing to apply the augmented-plane-wave (APW) method to this metal. As a preliminary, we have studied the group-theoretical properties of this substance, and the free-electron approximation to the energy bands and the Fermi surface.[2] It is known[3] that the free-electron approximation has proved to be a successful first approach to the energy bands of a number of elements, so that we may hope that it will give us a good enough indication of the nature of the gallium bands to guide us in interpreting the APW calculations when they are completed.

The crystal structure of gallium is orthorhombic,[4] with eight atoms in an orthorhombic cell. According to recent data of Barrett,[5] the sides of this cell, at 2.35°K, are $a=4.5151$ Å, $b=4.4881$ Å, $c=7.6318$ Å, respectively. It is an accident, without physical importance, that the two sides a and b are so nearly equal. According to earlier work of Bradley,[4] the eight atoms are located at the following positions:

$$(m,0,p,),\quad (m+\tfrac{1}{2},\tfrac{1}{2},\bar{p}),\quad (\bar{m}+\tfrac{1}{2},\tfrac{1}{2},p),\quad (\bar{m},0,\bar{p}),$$
$$(m,\tfrac{1}{2},p+\tfrac{1}{2}),\quad (m+\tfrac{1}{2},0,\bar{p}+\tfrac{1}{2}),\quad (\bar{m}+\tfrac{1}{2},0,p+\tfrac{1}{2}),$$
$$(\bar{m},\tfrac{1}{2},\bar{p}+\tfrac{1}{2}).\quad (1)$$

The values of the parameters m and p, according to Bradley, are $m=0.0785$, $p=0.1525$. These values were determined at room temperature, and we do not know whether they are correct at 2.35°K. However, nothing in our argument will depend on the precise values of these parameters.

* Assisted by the Office of Naval Research, the Army, Navy, and Air Force, and the National Science Foundation.

[1] We are indebted to Dr. B. W. Roberts, of the General Electric Company, for pointing out the importance of this problem to us.

[2] The free-electron Fermi surface has also been studied by Jules Marcus and W. A. Reed, preceding paper [Phys. Rev. **126**, 1298 (1962)]. We are indebted to Dr. Roberts and to Professor Marcus for information regarding this work.

[3] Much of the old work on energy bands was based on this approximation; see for instance N. F. Mott and H. Jones, *The Theory of the Properties of Metals and Alloys* (Oxford University Press, New York, 1936), Chap. V. More recent work includes that of F. Herman, Revs. Modern Phys. **30**, 102 (1958); W. A. Harrison, Phys. Rev. **116**, 555 (1959); **118**, 1182, 1190 (1960); contribution in *The Fermi Surface* (John Wiley & Sons, Inc., New York, 1960), p. 28.

[4] A. J. Bradley, Z. Krist. **91**, 302 (1935), who quotes earlier references.

[5] C. S. Barrett (private communication).

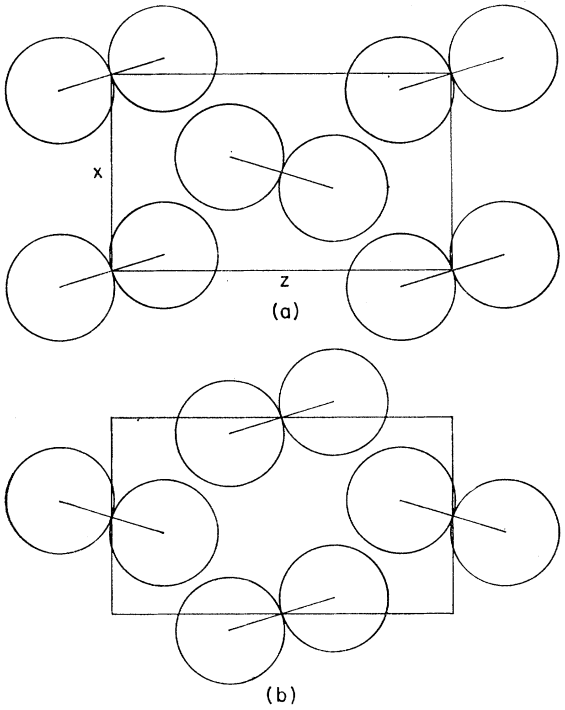

FIG. 1. Arrangement of atoms in (a) plane $y=0$; (b) plane $y=b/2$.

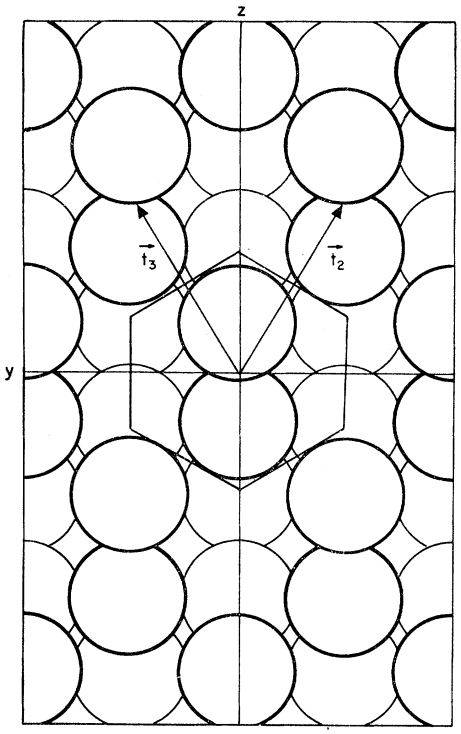

FIG. 2. Projection of atoms on yz plane. Heavily outlined atoms belong to molecules centered in plane $x=0$, lightly outlined atoms belong to molecules centered in plane $x=-a/2$. Translation vectors $\mathbf{t}_2$ and $\mathbf{t}_3$ are shown, also hexagonal Wigner-Seitz cell.

In Fig. 1 we show the xz plane, with the atoms located at $y=0$. These atoms may be considered to form diatomic molecules, as indicated in the figure; the atomic arrangement is the same as that found in the I_2 crystal. However, the distance between the two atoms in a molecule, 2.433 Å, is only slightly smaller than the distance from an atom in one molecule to the closest atom in another molecule. The shortest distance from an atom in one plane to another atom in the same plane not contained in the same molecule (as from the right-hand atom of the molecule centered at the origin to the left-hand atom of the molecule centered at $x=a/2$, $y=0$, $z=c/2$) is 2.704 Å, and the shortest distance from an atom in one plane to the closest atom in the neighboring plane (as from the right-hand atom of the molecule centered at the origin to the right-hand atom of the molecule centered at $x=a/2$, $y=b/2$, $z=0$) is 2.727 Å. One may surmise that the tendency of gallium to form diatomic molecules may explain its low melting point; presumably it melts into diatomic molecules.

The atoms in the plane at $y=b/2$ are shown in Fig. 1 (b). We see that this plane of atoms is like that at $y=0$, but displaced laterally. Hence there are only four differently located atoms in the unit cell, rather than eight. This is characteristic of the one-face-centered orthorhombic translation group, which we have in this case.[6] We can, then, choose a smaller unit cell than the orthorhombic cell ordinarily used, such that it will contain only four atoms. We shall achieve this if we take as primitive vectors the following quantities:

$$\begin{aligned}\mathbf{t}_1&=\mathbf{i}a,\\ \mathbf{t}_2&=\mathbf{j}b/2+\mathbf{k}c/2,\\ \mathbf{t}_3&=-\mathbf{j}b/2+\mathbf{k}c/2.\end{aligned}\tag{2}$$

Here $\mathbf{i}$, $\mathbf{j}$, $\mathbf{k}$ are unit vectors along the x, y, z axes. The vector $\mathbf{t}_1$ points from the molecule at the origin to that a distance a above it along x; $\mathbf{t}_2$ and $\mathbf{t}_3$ point from the origin to centers of the molecules in the plane $x=0$, at the bottom of the rectangle in Fig. 1 (b).

These vectors are better shown in Fig. 2, in which we project the atoms onto the yz plane. The vectors $\mathbf{t}_2$ and $\mathbf{t}_3$ are located in this plane. We can now set up a unit cell by the Wigner-Seitz construction. We take vectors from the origin to all equivalent points in the crystal, and take the planes which are the perpendicular bisectors of these vectors. Two of the planes bisect the vectors $\mathbf{t}_2$ and $\mathbf{t}_3$, two more bisect $-\mathbf{t}_2$ and $-\mathbf{t}_3$. Two more bisect the vectors of length b along the $\pm y$ directions. These planes cut the yz plane in the hexagon shown. In addition, we have planes perpendicular to the x axis, at heights $\pm a/2$. Taken together, these planes bound a hexagonal prism, which may be used as a unit cell. Two atoms are located entirely within the prism, others are located on the surface and shared

[6] See for example G. F. Koster, *Solid-State Physics* (Academic Press Inc., New York, 1957), Vol. V, pp. 173, 202. We have not followed in the present paper the notation used in this reference.

TABLE I. Operations of the point group with nonprimitive translations. The operations $R_1 \cdots R_8$ transform a function $\psi(x,y,z)$ into a transformed function $R_i\psi(x,y,z)$, as given in the table.

$\{\epsilon\|0\}$	$R_1\psi(x,y,z)=\psi(x,y,z)$
$\{\delta_2{}^a\|\boldsymbol{\tau}\}$	$R_2\psi(x,y,z)=\psi(x+\frac{1}{2}a, -y, -z+\frac{1}{2}c)$
$\{\delta_2{}^b\|0\}$	$R_3\psi(x,y,z)=\psi(-x, y, -z)$
$\{\delta_2{}^c\|\boldsymbol{\tau}\}$	$R_4\psi(x,y,z)=\psi(-x+\frac{1}{2}a, -y, z+\frac{1}{2}c)$
$\{i\|0\}$	$R_5\psi(x,y,z)=\psi(-x, -y, -z)$
$\{\sigma^a\|\boldsymbol{\tau}\}$	$R_6\psi(x,y,z)=\psi(-x+\frac{1}{2}a, y, z+\frac{1}{2}c)$
$\{\sigma^b\|0\}$	$R_7\psi(x,y,z)=\psi(x, -y, z)$
$\{\sigma^c\|\boldsymbol{\tau}\}$	$R_8\psi(x,y,z)=\psi(x+\frac{1}{2}a, y, -z+\frac{1}{2}c)$

with neighboring prisms, in such a way that the prism, whose volume is $abc/2$, half the rhombohedral cell, contains four atoms. The hexagon is not quite a regular hexagon, though it is very close to it. The atoms located on the surface are very nearly, but not quite, at the corners of the hexagon. It seems likely that the accidental relation between b and c, leading so nearly to a regular hexagon for this cell, is more significant in the structure than the fact that a and b are so nearly equal; a measures the height of the hexagon, while b is related to its dimensions in the basal plane.

The reciprocal vectors are given by the relation $\mathbf{t}_i \cdot \mathbf{b}_j = 2\pi\delta_{ij}$. They are

$$\begin{aligned} \mathbf{b}_1 &= (2\pi/a)\mathbf{i}, \\ \mathbf{b}_2 &= (2\pi/b)\mathbf{j} + (2\pi/c)\mathbf{k}, \\ \mathbf{b}_3 &= -(2\pi/b)\mathbf{j} + (2\pi/c)\mathbf{k}. \end{aligned} \tag{3}$$

When we set these vectors up in $\mathbf{k}$ space, and take the planes which form the perpendicular bisectors of the vectors to the points of the reciprocal lattice, we get the central Brillouin zone. The section of this zone in the k_yk_z plane is shown in Fig. 3, and a perspective drawing of it is given in Fig. 4. We see that it is also a hexagonal prism, rotated through 90° in the yz plane so that a point, rather than a flat surface, points to the right. We can see how close the hexagon is to a regular hexagon by noting that the boundary along the k_z direction comes at $2\pi/c = 0.8232$ Å^{-1}, while the boundary of one of the other faces of the hexagon comes at $[(\pi/b)^2+(\pi/c)^2]^{\frac{1}{2}} = 0.8120$ Å^{-1}. For comparison, the faces along the k_x direction come at a distance of $\pi/a = 0.6958$ Å^{-1}.

In Fig. 4, we have indicated symbols for the various symmetry directions which we shall encounter in our group-theoretical study. Since the problem is so similar to that of the hexagonal structure, we have followed where convenient the nomenclature of Herring[7] for that case. We must note, however, that unlike the hexagonal symmetry, the faces whose centers are indicated by Z and M in Fig. 4 have different symmetry properties, though they would be equivalent in the hexagonal case.

[7] C. Herring, J. Franklin Inst. **223**, 525 (1942).

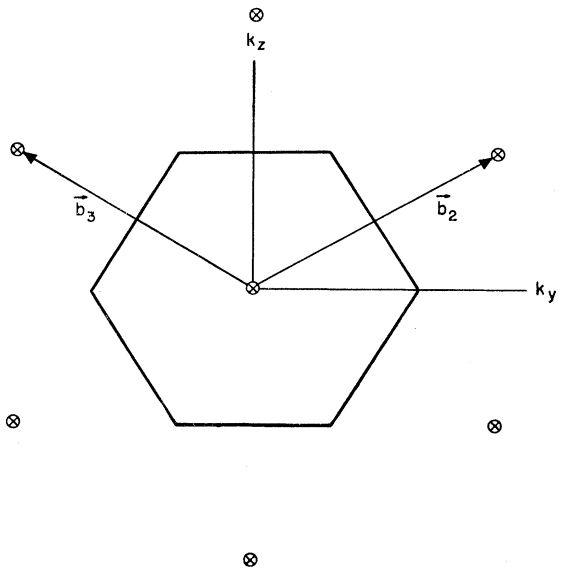

FIG. 3. Section of Brillouin zone in k_yk_z plane. The six closest points of the reciprocal lattice to the origin, in the yz plane, are shown. The next planes of lattice points above and below this plane, at $k_x = \pm 2\pi/a$, have the same arrangement in the k_yk_z plane as that shown above.

2. SYMMETRY OPERATIONS OF THE POINT AND SPACE GROUPS

The point group of this crystal is D_{2h}, with eight operations: the identity; rotations of 180° about the x, y, and z axes; the inversion; and reflection in the planes $x=0$, $y=0$, $z=0$. Half of these operations, namely the rotations about the x and z axes, and reflections in the planes $x=0$ and $z=0$, are accompanied by nonprimitive translations

$$\boldsymbol{\tau} = (a/2)\mathbf{i} + (c/2)\mathbf{k}. \tag{4}$$

We may describe these operations as in Table I, where we first describe the operations by symbols such as those introduced by Seitz,[8] and then give the effect of the

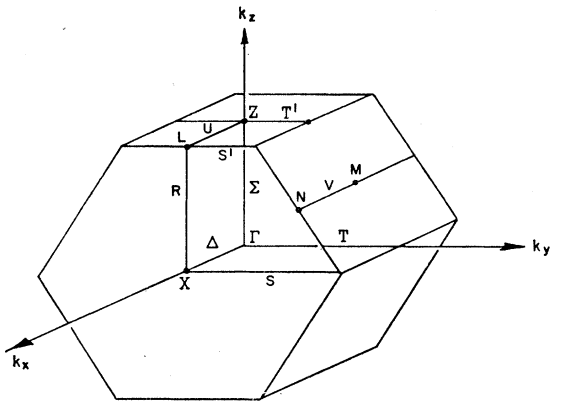

FIG. 4. Perspective drawing of central Brillouin zone, showing notations for various symmetry directions.

[8] F. Seitz, Z. Krist. **88**, 433 (1934); **90**, 289 (1935); **91**, 336 (1935); **94**, 100 (1936).

TABLE II. Characters of operations in the group of the wave vector at the points Γ, Z, X, and L in the gallium structure.

	R_1	R_2	R_3	R_4	R_5	R_6	R_7	R_8
Γ_1^+, Z_2^+	1	1	1	1	1	1	1	1
Γ_2^+, Z_1^+	1	−1	1	−1	1	−1	1	−1
Γ_3^+, Z_4^+	1	1	−1	−1	1	1	−1	−1
Γ_4^+, Z_3^+	1	−1	−1	1	1	−1	−1	1
Γ_1^-, Z_2^-	1	1	1	1	−1	−1	−1	−1
Γ_2^-, Z_1^-	1	−1	1	−1	−1	1	−1	1
Γ_3^-, Z_4^-	1	1	−1	−1	−1	−1	1	1
Γ_4^-, Z_3^-	1	−1	−1	1	−1	1	1	−1
X_1, L_1	2	0	0	0	0	0	2	0
X_2, L_2	2	0	0	0	0	0	−2	0

operations on an arbitrary function. The operations of the space group, D_{2h}^{18}, consist of one of the operations of Table I, combined with a translation

$$\mathbf{R}_n = n_1\mathbf{t}_1 + n_2\mathbf{t}_2 + n_3\mathbf{t}_3 = n_1 a\mathbf{i} + (n_2 - n_3)(b/2)\mathbf{j} + (n_2 + n_3)(c/2)\mathbf{k}, \quad (5)$$

where n_1, n_2, n_3 are integers.

Each of the operations of the point group belongs to a class by itself, and forms its own inverse. Hence each one transforms the wave vector $\mathbf{k}$ in the same way as the vector in ordinary space. For instance, R_2 transforms a wave vector with components k_x, k_y, k_z into a wave vector with components k_x, $-k_y$, $-k_z$. We can see this directly by letting the function ψ in Table I be an exponential representing a plane wave, $\exp[i(k_x x + k_y y + k_z z)]$. The transformed function, according to Table I, is

$$\exp\{i[k_x(x+\tfrac{1}{2}a) + k_y(-y) + k_z(-z+\tfrac{1}{2}c)]\} = \exp[i(k_x x - k_y y - k_z z)] \exp(i\mathbf{k}\cdot\boldsymbol{\tau}), \quad (6)$$

where $\boldsymbol{\tau}$ is given in Eq. (4). If in addition to the operation R_2 of Table I we included a translation $\mathbf{R}_n$, the combined operation would lead to an additional factor $\exp(i\mathbf{k}\cdot\mathbf{R}_n)$ in Eq. (6).

3. CHARACTER TABLES AND BASIS FUNCTIONS FOR PROPAGATION IN SYMMETRY DIRECTIONS

The star of wave vectors associated with a general point in k space consists of eight wave vectors, with components given by $\pm k_x$, $\pm k_y$, $\pm k_z$. The eight plane waves with these wave vectors form basis functions for an eight-dimensional irreducible representation of the space group. It is useful in discussing space groups to make use of the group-theoretical theorem that the sum of squares of the dimensionalities of all irreducible representations equals the number of operations in the space group, which is the product of the number of operations in the point group (in this case eight) and the number of independent translations $\mathbf{R}_n$ included within the repeating region of space determined by the periodic boundary conditions. We have as many reduced wave vectors as there are independent translations. Therefore, the theorem will be satisfied if the sum of squares of the dimensionalities of the irreducible representations arising from the wave vectors in a star equals the number of wave vectors in the star, multiplied by the number of operations in the point group, in this case eight. For a general point, where we have eight wave vectors in the star, the sum of the squares of the dimensionalities will be eight times the number of vectors in the star, or 64. Since we have one 8-dimensional irreducible representation, the theorem checks. The theorem is trivial in this case, but is a very useful check on the more involved cases which we find at various symmetry points. The theorem is proved in Appendix I.

Now let us take up these symmetry points. First we must have a notation for the wave vector which distinguishes the reduced wave vector, within the central Brillouin zone, from the remaining part of the wave vector, which represents a vector of the reciprocal lattice. We shall use $\mathbf{k}$ for the reduced wave vector, $\mathbf{K}$ for the vector of the reciprocal lattice, where

$$\mathbf{K} = p_1\mathbf{b}_1 + p_2\mathbf{b}_2 + p_3\mathbf{b}_3 = (2\pi/a)p_1\mathbf{i} + (2\pi/b)(p_2 - p_3)\mathbf{j} + (2\pi/c)(p_2 + p_3)\mathbf{k} \quad (7)$$

and where p_1, p_2, p_3 are integers. We then denote the whole wave vector by $\mathbf{k}+\mathbf{K}$.

We are now ready to take up the first symmetry point, Γ, or $\mathbf{k}=0$, so that the wave vector is $\mathbf{K}$. There is only one vector forming the star, namely $\mathbf{k}=0$, so that the sum of squares of the dimensionalities of the irreducible representation is 8. The point group of the wave vector is the complete group D_{2h} formed from all of the operators given in Table I. We know that this group has eight one-dimensional irreducible representations, checking our statement regarding the sum of squares of dimensionalities. In Table II we give the character table for these irreducible representations, and in Table III we give basis functions in the form of symmetrized plane waves. A general basis function would consist of a linear combination of all symmetrized plane waves of the type given in Table III, for all values of K_x, K_y, K_z consistent with Eq. (7), each with an arbitrary coefficient. It is useful to have such expressions in terms of symmetrized plane waves, to investigate the physical form of the wave function, and to compare with wave functions set up by the augmented plane wave or orthogonalized plane wave method, which will result in the same symmetry types. In Table II we give also the characters at the points Z, X, and L.

It is easy to verify the entries of Tables II and III by direct calculation. As an example, let us verify the fact that the character for the operation R_2, for the irreducible representation Γ_2^+, is -1. From Table III we see that there are two sorts of basis functions in this case, depending on whether the quantity $\exp(i\mathbf{K}\cdot\boldsymbol{\tau})$ equals 1 or -1. It must have one or the other of these

TABLE III. Symmetrized plane wave basis functions for various symmetry directions, gallium structure.

$\exp(i\mathbf{K}\cdot\boldsymbol{\tau})$ 1	$\exp(i\mathbf{K}\cdot\boldsymbol{\tau})$ -1	
Γ_1^+	Γ_2^+	$\cos(K_x x)\cos(K_y y)\cos(K_z z)$
Γ_2^+	Γ_1^+	$\sin(K_x x)\cos(K_y y)\sin(K_z z)$
Γ_3^+	Γ_4^+	$\cos(K_x x)\sin(K_y y)\sin(K_z z)$
Γ_4^+	Γ_3^+	$\sin(K_x x)\sin(K_y y)\cos(K_z z)$
Γ_1^-	Γ_2^-	$\sin(K_x x)\sin(K_y y)\sin(K_z z)$
Γ_2^-	Γ_1^-	$\cos(K_x x)\sin(K_y y)\cos(K_z z)$
Γ_3^-	Γ_4^-	$\sin(K_x x)\cos(K_y y)\cos(K_z z)$
Γ_4^-	Γ_3^-	$\cos(K_x x)\cos(K_y y)\sin(K_z z)$
Z_1^+	Z_2^+	$\cos(K_x x)\cos(K_y y)\cos[(2\pi/c+K_z)z]$
Z_2^+	Z_1^+	$\sin(K_x x)\cos(K_y y)\sin[(2\pi/c+K_z)z]$
Z_3^+	Z_4^+	$\cos(K_x x)\sin(K_y y)\sin[(2\pi/c+K_z)z]$
Z_4^+	Z_3^+	$\sin(K_x x)\sin(K_y y)\cos[(2\pi/c+K_z)z]$
Z_1^-	Z_2^-	$\sin(K_x x)\sin(K_y y)\sin[(2\pi/c+K_z)z]$
Z_2^-	Z_1^-	$\cos(K_x x)\sin(K_y y)\cos[(2\pi/c+K_z)z]$
Z_3^-	Z_4^-	$\sin(K_x x)\cos(K_y y)\cos[(2\pi/c+K_z)z]$
Z_4^-	Z_3^-	$\cos(K_x x)\cos(K_y y)\sin[(2\pi/c+K_z)z]$
Δ_1	Δ_2	$\exp[i(k_x+K_x)x]\cos(K_y y)\cos(K_z z)$
Δ_2	Δ_1	$\exp[i(k_x+K_x)x]\cos(K_y y)\sin(K_z z)$
Δ_3	Δ_4	$\exp[i(k_x+K_x)x]\sin(K_y y)\sin(K_z z)$
Δ_4	Δ_3	$\exp[i(k_x+K_x)x]\sin(K_y y)\cos(K_z z)$
U_1	U_2	$\exp[i(k_x+K_x)x]\cos(K_y y)\cos[(2\pi/c+K_z)z]$
U_2	U_1	$\exp[i(k_x+K_x)x]\cos(K_y y)\sin[(2\pi/c+K_z)z]$
U_3	U_4	$\exp[i(k_x+K_x)x]\sin(K_y y)\sin[(2\pi/c+K_z)z]$
U_4	U_3	$\exp[i(k_x+K_x)x]\sin(K_y y)\cos[(2\pi/c+K_z)z]$
T_1	T_2	$\cos(K_x x)\exp[i(k_y+K_y)y]\cos(K_z z)$
T_2	T_1	$\sin(K_x x)\exp[i(k_y+K_y)y]\sin(K_z z)$
T_3	T_4	$\cos(K_x x)\exp[i(k_y+K_y)y]\sin(K_z z)$
T_4	T_3	$\sin(K_x x)\exp[i(k_y+K_y)y]\cos(K_z z)$
T_1'	T_2'	$\sin(K_x x)\exp[i(k_y+K_y)y]\sin[(2\pi/c+K_z)z]$
T_2'	T_1'	$\cos(K_x x)\exp[i(k_y+K_y)y]\cos[(2\pi/c+K_z)z]$
T_3'	T_4'	$\sin(K_x x)\exp[i(k_y+K_y)y]\cos[(2\pi/c+K_z)z]$
T_4'	T_3'	$\cos(K_x x)\exp[i(k_y+K_y)y]\sin[(2\pi/c+K_z)z]$
Σ_1	Σ_2	$\cos(K_x x)\cos(K_y y)\exp[i(k_z+K_z)z]$
Σ_2	Σ_1	$\sin(K_x x)\cos(K_y y)\exp[i(k_z+K_z)z]$
Σ_3	Σ_4	$\cos(K_x x)\sin(K_y y)\exp[i(k_z+K_z)z]$
Σ_4	Σ_3	$\sin(K_x x)\sin(K_y y)\exp[i(k_z+K_z)z]$
N_1	N_2	$\cos[(\pi/a+K_x)x]\cos[(\pi/b+K_y)y+(\pi/c+K_z)z]$ $+i\sin[(\pi/a+K_x)x]\sin[(\pi/b+K_y)y+(\pi/c+K_z)z]$
N_2	N_1	$\cos[(\pi/a+K_x)x]\cos[(\pi/b+K_y)y+(\pi/c+K_z)z]$ $-i\sin[(\pi/a+K_x)x]\sin[(\pi/b+K_y)y+(\pi/c+K_z)z]$
N_3	N_4	$\sin[(\pi/a+K_x)x]\cos[(\pi/b+K_y)y+(\pi/c+K_z)z]$ $-i\cos[(\pi/a+K_x)x]\sin[(\pi/b+K_y)y+(\pi/c+K_z)z]$
N_4	N_3	$\sin[(\pi/a+K_x)x]\cos[(\pi/b+K_y)y+(\pi/c+K_z)z]$ $+i\cos[(\pi/a+K_x)x]\sin[(\pi/b+K_y)y+(\pi/c+K_z)z]$
V_1	V_2	$\exp[i(k_x+K_x)x]\{\cos[(\pi/b+K_y)y+(\pi/c+K_z)z]$ $+\sin[(\pi/b+K_y)y+(\pi/c+K_z)z]\}$
V_2	V_1	$\exp[i(k_x+K_x)x]\{\cos[(\pi/b+K_y)y+(\pi/c+K_z)z]$ $-\sin[(\pi/b+K_y)y+(\pi/c+K_z)z]\}$

$\exp(iK_z c/2)$ [note difference from $\exp(i\mathbf{K}\cdot\boldsymbol{\tau})$]

1	-1	
R_1	R_2	$\cos[(\pi/a+K_x)(x+a/4)]\cos(K_y y)\exp[i(k_z+K_z)z]$
R_2	R_1	$\sin[(\pi/a+K_x)(x+a/4)]\cos(K_y y)\exp[i(k_z+K_z)z]$
R_3	R_4	$\cos[(\pi/a+K_x)(x+a/4)]\sin(K_y y)\exp[i(k_z+K_z)z]$
R_4	R_3	$\sin[(\pi/a+K_x)(x+a/4)]\sin(K_y y)\exp[i(k_z+K_z)z]$
H_1	H_2	$\cos[(\pi/a+K_x)(x+a/4)]\exp\{i[(k_y+K_y)y+(k_z+K_z)z]\}$
H_2	H_1	$\sin[(\pi/a+K_x)(x+a/4)]\exp\{i[(k_y+K_y)y+(k_z+K_z)z]\}$

Two-dimensional representations

X_1	$\exp[i(\pi/a+K_x)x]\cos(K_y y)\cos(K_z z)$	$\exp[-i(\pi/a+K_x)x]\cos(K_y y)\cos(K_z z)$
X_1	$\exp[i(\pi/a+K_x)x]\cos(K_y y)\sin(K_z z)$	$\exp[-i(\pi/a+K_x)x]\cos(K_y y)\sin(K_z z)$
X_2	$\exp[i(\pi/a+K_x)x]\sin(K_y y)\cos(K_z z)$	$\exp[-i(\pi/a+K_x)x]\sin(K_y y)\cos(K_z z)$
X_2	$\exp[i(\pi/a+K_x)x]\sin(K_y y)\sin(K_z z)$	$\exp[-i(\pi/a+K_x)x]\sin(K_y y)\sin(K_z z)$
L_1	$\cos[(\pi/a+K_x)(x+a/4)]\cos(K_y y)\exp[i(2\pi/c+K_z)z]$	$\sin[(\pi/a+K_x)(x+a/4)]\cos(K_y y)\exp[-i(2\pi/c+K_z)z]$
L_1	$\sin[(\pi/a+K_x)(x+a/4)]\cos(K_y y)\exp[i(2\pi/c+K_z)z]$	$\cos[(\pi/a+K_x)(x+a/4)]\cos(K_y y)\exp[-i(2\pi/c+K_z)z]$
L_2	$\cos[(\pi/a+K_x)(x+a/4)]\sin(K_y y)\exp[i(2\pi/c+K_z)z]$	$\sin[(\pi/a+K_x)(x+a/4)]\sin(K_y y)\exp[-i(2\pi/c+K_z)z]$
L_2	$\sin[(\pi/a+K_x)(x+a/4)]\sin(K_y y)\exp[i(2\pi/c+K_z)z]$	$\cos[(\pi/a+K_x)(x+a/4)]\sin(K_y y)\exp[-i(2\pi/c+K_z)z]$
S_1	$\cos[(\pi/a+K_x)(x+a/4)]\exp[i(k_y+K_y)y]\cos(K_z z)$	$\sin[(\pi/a+K_x)(x+a/4)]\exp[i(k_y+K_y)y]\cos(K_z z)$
S_1	$\cos[(\pi/a+K_x)(x+a/4)]\exp[i(k_y+K_y)y]\sin(K_z z)$	$\sin[(\pi/a+K_x)(x+a/4)]\exp[i(k_y+L_y)y]\sin(K_z z)$
S_1'	$\cos[(\pi/a+K_x)(x+a/4)]\exp[i(k_y+K_y)y]\cos[(2\pi/c+K_z)z]$	$\sin[(\pi/a+K_x)(x+a/4)]\exp[i(k_y+K_y)y]\cos[(2\pi/c+K_z)z]$
S_1'	$\cos[(\pi/a+K_x)(x+a/4)]\exp[i(k_y+K_y)y]\sin[(2\pi/c+K_z)z]$	$\sin[(\pi/a+K_x)(x+a/4)]\exp[i(k_y+K_y)y]\sin[(2\pi/c+K_z)z]$
M_1	$\cos(K_x x)\exp\{i[(\pi/b+K_y)y+(\pi/c+K_z)z]\}$	$\cos(K_x x)\exp\{-i[(\pi/b+K_y)y+(\pi/c+K_z)z]\}$
M_1	$\sin(K_x x)\exp\{i[(\pi/b+K_y)y+(\pi/c+K_z)z]\}$	$\sin(K_x x)\exp\{-i[(\pi/b+K_y)y+(\pi/c+K_z)z]\}$

values, for if we combine Eqs. (4) and (7), we see that it equals

$$\exp(i\mathbf{K}\cdot\boldsymbol{\tau})=\exp[\pi i(p_1+p_2+p_3)] \tag{8}$$

which must be ± 1, since the p's are integers. Let us choose the case where it equals -1. Then from Table III we see that a basis function is $\cos K_x x\cos K_y y\cos K_z z$. Let us now operate on this function with the operator R_2, which means that we replace x by $x+a/2$, y by $-y$, z by $-z+c/2$. The function then becomes

$$\cos[K_x(x+a/2)]\cos(K_y y)\cos[K_z(z-c/2)]$$
$$=\cos(K_x x)\cos(K_y y)\cos(K_z z)\cos(\pi p_1)$$
$$\times\cos[\pi(p_2+p_3)] \tag{9}$$

where we have used Eq. (7). Now $\cos(\pi p_1)$, where p_1

TABLE IV. Characters of operations in the group of the wave vector at the points Δ, U, in the gallium structure.

	R_2	R_2	R_7	R_8
Δ_1, U_1	1	$\exp(i\mathbf{k}\cdot\boldsymbol{\tau})$	1	$\exp(i\mathbf{k}\cdot\boldsymbol{\tau})$
Δ_2, U_2	1	$-\exp(i\mathbf{k}\cdot\boldsymbol{\tau})$	1	$-\exp(i\mathbf{k}\cdot\boldsymbol{\tau})$
Δ_3, U_3	1	$\exp(i\mathbf{k}\cdot\boldsymbol{\tau})$	-1	$-\exp(i\mathbf{k}\cdot\boldsymbol{\tau})$
Δ_4, U_4	1	$-\exp(i\mathbf{k}\cdot\boldsymbol{\tau})$	-1	$\exp(i\mathbf{k}\cdot\boldsymbol{\tau})$

is an integer, equals 1 if p_1 is even, -1 if p_1 is odd, so that it equals $\exp(\pi i p_1)$. Similarly $\cos[\pi(p_2+p_3)]=\exp[\pi i(p_2+p_3)]$. Hence, $\cos(\pi p_1)\cos[\pi(p_2+p_3)]=\exp[\pi i(p_1+p_2+p_3)]=\exp(i\mathbf{K}\cdot\boldsymbol{\tau})$. Since we have taken the case where this is -1, we see from Eq. (9) that the effect of operating on our basis function with R_2 is to multiply it by -1, as we wished to show. Similar proofs hold in all cases.

Next we consider propagation along the x axis, the direction Δ. The group of the wave vector consists of the operations R_1, R_2, R_7, R_8, which as we see from Table I leave the sign of x unchanged, and hence leave k_x unchanged. The point group is C_{2v}, with four one-dimensional irreducible representations. There are now two wave vectors in the star, the reduced wave vectors k_x and $-k_x$, so that each one-dimensional irreducible representation of the point group goes into a two-dimensional irreducible representation of the space group. The sum of squares of the dimensionalities is then $4(2^2)=16$, 8 times the number of vectors forming the star, verifying the general theorem quoted at the beginning of this section. We shall not repeat the verifications of this theorem in further cases which we shall take up, but the reader can easily carry out these checks on the correctness of the analysis. The character table is given in Table IV, and basis functions are given in Table III.

As in the case of the point Γ, these entries are easily verified by direct use of the operators on the basis functions. A similar situation is found at the other symmetry points, and we give character tables and basis functions for them in Tables III, V–VIII.

One particularly important result of the study of the symmetry behavior of wave functions is to find the degenerate representations, showing in what cases energy bands must stick together on account of symmetry. We find two-dimensional irreducible representations at X, S, S', L, and M. In addition to these cases

TABLE V. Characters of operations in the group of the wave vector at the points T, T', S, S', in the gallium structure.

	R_1	R_3	R_6	R_8
T_1, T_1'	1	1	1	1
T_2, T_2'	1	1	-1	-1
T_3, T_3'	1	-1	1	-1
T_4, T_4'	1	-1	-1	1
S_1, S_1'	2	0	0	0

TABLE VI. Characters of operations in the group of the wave vector at the points Σ, R in the gallium structure. (Do not confuse operators R_1, R_4, R_6, R_7 with representations R_1, R_2, R_3, R_4.)

	R_1	R_4	R_6	R_7
Σ_1	1	$\exp(i\mathbf{k}\cdot\boldsymbol{\tau})$	$\exp(i\mathbf{k}\cdot\boldsymbol{\tau})$	1
Σ_2	1	$-\exp(i\mathbf{k}\cdot\boldsymbol{\tau})$	$-\exp(i\mathbf{k}\cdot\boldsymbol{\tau})$	1
Σ_3	1	$-\exp(i\mathbf{k}\cdot\boldsymbol{\tau})$	$\exp(i\mathbf{k}\cdot\boldsymbol{\tau})$	-1
Σ_4	1	$\exp(i\mathbf{k}\cdot\boldsymbol{\tau})$	$-\exp(i\mathbf{k}\cdot\boldsymbol{\tau})$	-1
R_1	1	$i\exp(i\mathbf{k}\cdot\boldsymbol{\tau})$	$i\exp(i\mathbf{k}\cdot\boldsymbol{\tau})$	1
R_2	1	$-i\exp(i\mathbf{k}\cdot\boldsymbol{\tau})$	$-i\exp(i\mathbf{k}\cdot\boldsymbol{\tau})$	1
R_3	1	$-i\exp(i\mathbf{k}\cdot\boldsymbol{\tau})$	$i\exp(i\mathbf{k}\cdot\boldsymbol{\tau})$	-1
R_4	1	$i\exp(i\mathbf{k}\cdot\boldsymbol{\tau})$	$-i\exp(i\mathbf{k}\cdot\boldsymbol{\tau})$	-1

in which two levels must be degenerate on account of the properties of the irreducible representations, we have several additional cases of degeneracy arising on account of time reversal. These cases are found at R, N, at a general point of the hexagonal face, denoted by H, and at V. We thus see that, as in the hexagonal structure, all energy levels are twofold degenerate on the hexagonal face. Also they are twofold degenerate all along the line V (which includes the case M, where the degeneracy arises from the properties of the irreducible representation of the space group).

We can easily verify the time-reversal degeneracy in these cases, from the basis functions which are given in Table III. The operation of time reversal replaces the wave function by its complex conjugate. If in addition we apply the inversion, our operation R_5, the reduced wave vector remains unchanged, so that this combined operation belongs to the group of the wave vector, when time reversal is included. If this combined operation applied to one of the basis functions produces the basis function for another irreducible representation, these two representations must be connected with wave functions which are degenerate with each other.

The only cases where this leads to additional degeneracy are enumerated above. At R, we find that the time-reversal plus inversion operations changes the first basis function $\cos[(\pi/a+K_x)(x+a/4)]\cos(K_y y)\times\exp[i(k_z+K_z)z]$ into plus or minus the second function, $\sin[(\pi/a+K_x)(x+a/4)]\cos(K_y y)\exp[i(k_z+K_z)z]$. Hence these two functions correspond to the same energy, showing that the one-dimensional irreducible representations R_1 and R_2 must be degenerate. Similarly we can show that R_3 and R_4 must be degenerate. We find by the same argument that N_1 and N_2 are de-

TABLE VII. Characters of operations in the group of the wave vector at the points N, M in the gallium structure.

	R_1	R_2	R_5	R_6
N_1	1	i	1	i
N_2	1	$-i$	1	$-i$
N_3	1	i	-1	$-i$
N_4	1	$-i$	-1	i
M_1	2	0	0	0

TABLE VIII. Characters of operations in the group of the wave vector at the points H, a general point in the hexagonal face, and V, in the gallium structure.

	R_1	R_6
H_1	1	$i\exp(i\mathbf{k}\cdot\boldsymbol{\tau})$
H_2	1	$-i\exp(i\mathbf{k}\cdot\boldsymbol{\tau})$
	R_1	R_2
V_1	1	$-i\exp(i\mathbf{k}\cdot\boldsymbol{\tau})$
V_2	1	$i\exp(i\mathbf{k}\cdot\boldsymbol{\tau})$

generate, N_3 and N_4; the two representations H_1 and H_2 at a general point of the hexagonal face are degenerate; and V_1 and V_2 are degenerate.

By inspection of the character tables, or of the basis functions, it is simple to establish the compatibility relations between symmetry types in different symmetry points. These relations are given in Table IX.

TABLE IX. Compatibility relations between irreducible representations for different symmetry directions, gallium structure.

Γ_1^+	Γ_2^+	Γ_3^+	Γ_4^+	Γ_1^-	Γ_2^-	Γ_3^-	Γ_4^-	X_1	X_2
Δ_1	Δ_2	Δ_3	Δ_4	Δ_3	Δ_4	Δ_1	Δ_2	Δ_1	Δ_3
T_1	T_2	T_3	T_4	T_2	T_1	T_4	T_3	Δ_2	Δ_4
Σ_1	Σ_2	Σ_3	Σ_4	Σ_4	Σ_3	Σ_2	Σ_1	R_1	R_3
								R_2	R_4
Z_1^+	Z_2^+	Z_3^+	Z_4^+	Z_1^-	Z_2^-	Z_3^-	Z_4^-	S_1	S_1
U_1	U_2	U_3	U_4	U_3	U_4	U_1	U_2		
T_2'	T_1'	T_4'	T_3'	T_1'	T_2'	T_3'	T_4'	L_1	L_2
Σ_1	Σ_2	Σ_3	Σ_4	Σ_4	Σ_3	Σ_2	Σ_1	U_1	U_3
								U_2	U_4
T_1	T_2	T_3	T_4			M_1		R_1	R_3
T_1'	T_2'	T_3'	T_4'			V_1		R_2	R_4
						V_2		S_1'	S_1'
N_1	N_2	N_3	N_4						
V_1	V_2	V_1	V_2						
R_1	R_2	R_3	R_4						
H_1	H_2	H_1	H_2						

4. ENERGY BANDS IN THE FREE ELECTRON APPROXIMATION

We have mentioned[3] that the free-electron approximation has been found to give a fairly good first approximation to the energy bands of a number of metals. Therefore in the present section we shall examine the results of this approximation for gallium. We are to assume that the energy is given by

$$\text{Energy}=(\hbar^2/2m)[(k_x+K_x)^2+(k_y+K_y)^2+(k_z+K_z)^2]. \quad (10)$$

It is convenient in working out the energy bands by this method to start at the point Γ, $\mathbf{k}=0$. Then we can set up different combinations of the quantities K_x, K_y, K_z, according to Eq. (7), and get the energies of the various states of symmetry Γ. For each combination of K's, there will be only definite symmetry orbitals which are nonvanishing, as we can find from Table III. Hence we can immediately find the energy levels, and symmetries, found at $\mathbf{k}=0$.

This calculation, for the lower energy levels, is given in Table X. The first entry, for $E=0$, corresponds to $K_x=K_y=K_z=0$. As we can see from Table III, the only nonvanishing basis function will be the first one listed, corresponding to Γ_1^+, since each other function has a sine, which vanishes. For the second entry, we have $K_x=\pm 2\pi/a$, $K_y=K_z=0$. Hence, in Table III we must have the factor $\cos(K_y y)\cos(K_z z)$, but we may have either $\cos(K_x x)$ or $\sin(K_x x)$, so that, since in this case $\exp(i\mathbf{K}\cdot\boldsymbol{\tau})=-1$, we may have either Γ_2^+ or Γ_4^-. Similar arguments apply in each entry in the table.

It is now easy, starting with this point Γ, to proceed along the x, y, or z directions, using Eq. (10) for the energy, and get the energy as a function of $\mathbf{k}$. When we reach the edge of the Brillouin zone, we can proceed along the surface of the zone. In each case we may find the symmetries of the states resulting by use of the compatibility relations, Table IX, or by working out the basis functions. In Fig. 5 we give the resulting energy as a function of $\mathbf{k}$, for a good many of the symmetry directions, plotting in the way used by Herman[3] in discussion of the free-electron approximation. To avoid confusion, we have indicated the symmetry types at the points Γ and Z only on the boundaries of the figure, and we have not given a scale of energy. The horizontal line approximately half way up the diagram represents the Fermi energy, which comes at 0.7739 ry, or 10.53 ev; this establishes the energy scale.

TABLE X. Energy levels and their symmetries for $\mathbf{k}=0$, gallium. Free-electron approximation. Energies in ry.

p_1	p_2	p_3	$K_x a/2\pi$	$K_y b/2\pi$	$K_z c/2\pi$	Energy	$\exp(i\mathbf{K}\cdot\boldsymbol{\tau})$	Symmetries
0	0	0	0	0	0	0.0000	1	Γ_1^+
±1	0	0	±1	0	0	0.5422	−1	Γ_2^+, Γ_4^-
0	±1	0	0	±1	±1	0.7386	−1	Γ_2^+, Γ_4^+, Γ_1^-, Γ_3^-
0	0	±1						
0	1	1	0	0	±2	0.7592	1	Γ_1^+, Γ_4^-
0	−1	−1						
±1	±1	0	±1	±1	±1	1.2808	1	Γ_1^+, Γ_2^+, Γ_3^+, Γ_4^+
±1	0	±1						Γ_1^-, Γ_2^-, Γ_3^-, Γ_4^-
±1	1	1	±1	0	±2	1.3014	−1	Γ_1^+, Γ_2^+, Γ_3^-, Γ_4^-
±1	−1	−1						

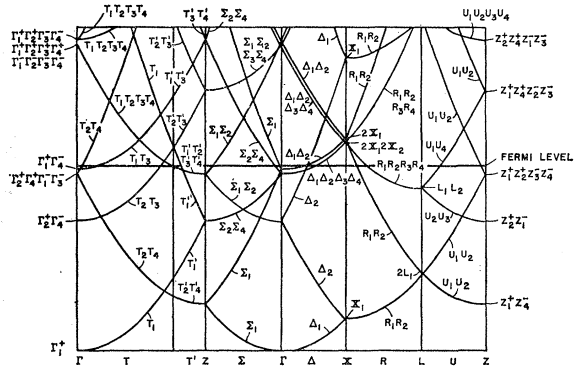

FIG. 5. Energy as function of $\mathbf{k}$, in symmetry directions, free-electron approximation for gallium. Horizontal line, Fermi energy=0.7739 ry=10.53 ev. (Note an error in the figure: The states labeled U_1, U_4 going to the lowest Z_1^+, Z_4^-, should be U_1, U_2.)

Perhaps the most striking feature of Fig. 5 is the complication of the figure in the neighborhood of the Fermi energy, and the widely varying number of energy bands occupied in different parts of the Brillouin zone. For example, as we go along the direction T, from Γ to the boundary of the zone, where the direction changes to T', we see that we start at Γ with nine occupied bands, namely the T_1 arising from the lowest level at Γ, T_2 and T_3 arising from the second level, two T_2's and two T_4's from the third level, and T_1 and T_3 from the fourth level. As we go along T, the T_2 and T_4 forming the upper branch arising from the third level at Γ rise above the Fermi level, leaving seven occupied bands. Next the T_1 and T_3 rise above the Fermi level, leaving five bands, and finally the T_2 and T_3 rise above the Fermi level, leaving only three occupied bands at the edge of the Brillouin zone. Similar situations arise in other symmetry directions. It is obvious that relatively small departures from the free-electron bands shown in Fig. 5 could make a profound change in this situation, so that we should not trust the free-electron predictions very far.

Nevertheless, it is interesting to investigate the predictions of the free-electron approximation regarding the Fermi surface of gallium, since this is what is needed to compare with most of the experiments. Such an investigation has been made by Marcus and Reed,[2] and for that reason we shall not go into great details in describing the results. To carry out the construction, we must draw Fermi spheres centered on each of the points shown in Fig. 3, and on corresponding points in the layers above and below the one shown in Fig. 3, in the reciprocal space. These can be easily seen to be the only Fermi spheres which will cut through the central Brillouin zone. These spheres, in the central zone, form parts of the various Fermi surfaces.

It is not always realized clearly just what is the nature of the Fermi surface, in a complicated case like the present. At each point of the central Brillouin zone, there will be a definite number of occupied energy bands, whose energies lie below the Fermi energy. Thus, we have just seen that as we go along the line T, from Γ to the boundary of the zone, this number of occupied bands is successively 9, 7, 5, and 3. There is a Fermi surface separating the regions where the number of occupied bands has one integral value or the next. Thus, in the present problem, we find that there are parts of the Brillouin zone having each number of occupied bands from 2 to 9, inclusive. Hence, there is a 2–3 Fermi surface (separating the regions where there are two and three occupied bands respectively), a 3–4 surface, and so on, up to an 8–9 surface. These would be referred to as the third band surface, fourth band surface, and so on up to the ninth band surface, in the language used by Harrison, Marcus, and Reed.[2,3] The same situation will be found with the true solutions of the periodic potential problem, as well as with the free-electron approximation. This complicated situation contrasts with the very simple situation found in an alkali metal, where part of the Brillouin zone has one occupied band, part has none, and the only Fermi surface is the one which would be denoted as 0–1, or the first band surface. Each of these Fermi surfaces, which in general will be independent of each other, can be concerned in such phenomena as the de Haas-van Alphen effect, magnetoresistance, and so on.

The Fermi surfaces in the present case are shown in Fig. 6, where we show sections through the Brillouin zone made by planes perpendicular to the x axis. These surfaces could be shown in perspective, but we shall omit doing so, since Marcus and Reed will present such drawings. In Fig. 6, we have divided the Brillouin zone from Γ to X into ten equal intervals, and have shown the corresponding sections of the Fermi surfaces. For ease in understanding the situation, we have given two sets of sections, one indicating the areas where there are 9, 8, 7, and 6 or less bands, and the other showing the areas where there are 6 or more, 5, 4, 3, or 2 occupied bands.

If gallium were a semiconductor, there would be six occupied bands, since there are four atoms per unit cell, each containing three outer electrons, or a total of twelve electrons per unit cell, occupying six bands with the two spin directions. In some respects it is more like a semimetal. We are familiar with cases in which there are some parts of the Brillouin zone where there are more occupied bands than in a semiconductor, with compensating regions where there are fewer. In the former regions, we should speak of conduction bands containing some electrons, if we were dealing with a semiconductor, and in the latter regions there would be holes left in the valence bands. Here in a sense we may regard the large parts of the Brillouin zone where there are six occupied bands as the normal situation, resembling a semiconductor. The regions where more than six bands are occupied correspond to occupied conduction bands in a semimetal, while those where fewer than

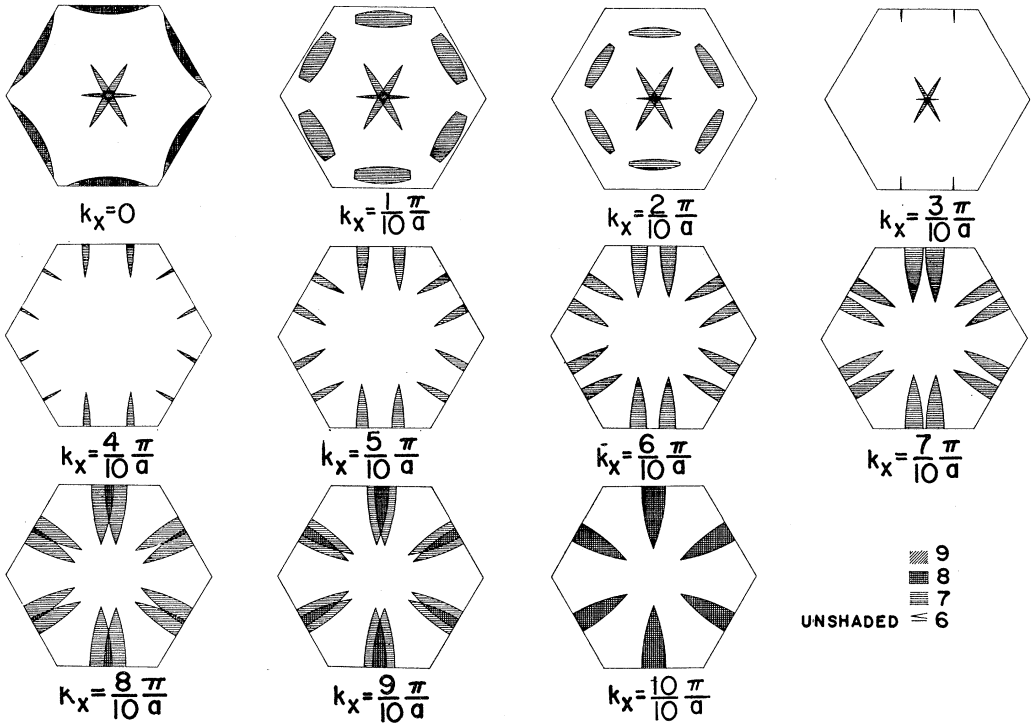

(a)

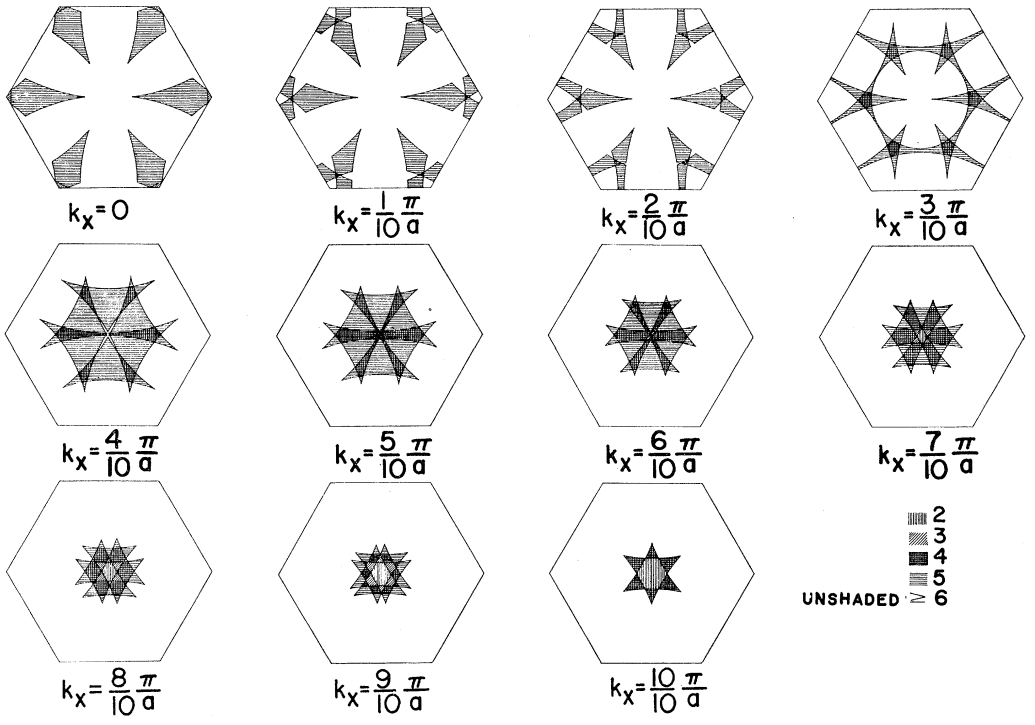

(b)

FIG. 6. Intersections of Fermi surfaces with planes from $k_x=0$ to boundary of Brillouin zone. First set of sections, surfaces corresponding to six or more bands. Second set, six or less bands.

six bands are occupied correspond to holes in a valence band.

It is interesting to examine the various Fermi surfaces more in detail from Fig. 6. The reader will, in the first place, be able to compare the situation with Fig. 5. For instance, the case which we discussed above, namely the line T, corresponds to the horizontal line passing through the middle of the hexagonal sections for $k_x=0$, in Fig. 6. In the first section shown, corresponding to six to nine bands, we see that we start at Γ with nine bands, then go down to seven. In the section corresponding to two to six bands, for $k_x=0$, we see the large range of this horizontal line where there are five bands (this starts in fact where the region of seven bands leaves off), and the small segment at the corner of the Brillouin zone where there are three bands.

The next interesting feature of Fig. 6 concerns the general topological properties of the various Fermi surfaces. The 6–7 surface, or seventh band surface, for instance, consists of a number of isolated segments, including the star-shaped solid at the center of the Brillouin zone, and isolated solids of various shapes on the surfaces of the zone, extending from one zone into the next, but not multiply connected. In contrast, the 5–6 surface, or sixth band surface, shows a very complicated multiple connectivity. In the plane $k_x=0$ we have six pointed spearlike sections pointing toward the origin. As we increase k_x, these merge, so that at $k_x=3\pi/10a$ there is a complicated structure like a crown with stars, extending throughout space. This detaches itself from the next Brillouin zone as k_x increases, leading to an isolated surface near the origin. This, however, maintains itself at the top of the Brillouin zone, and as we go into the next higher zone, it is attached to an inverted version of the same sequence of shapes, showing that there is a multiple connectivity along the x direction, as well as in planes at right angles to this direction. Since it is known[9] that multiple connectivity of the Fermi surface has important implications for magnetoresistance and other properties, this property of the Fermi surfaces related to hole conduction, which seems well enough established so that it very likely would persist in the true Fermi surface, seems likely to be important experimentally.

We may now ask which features of the Fermi surfaces as determined by the free-electron model are likely to be found for the true Fermi surface as well. We shall probably find the same general sort of surfaces, though the sharp points found in Fig. 6 will normally be rounded off. One feature of Fig. 6 arises from the free-electron model: the way in which in many cases the number of bands jumps by two units from one area to the next, rather than by one unit at a time. This is in general a result of accidental degeneracies introduced by the model. The only cases where this situation must be expected, for the true surfaces, are those where twofold degeneracy is required by symmetry: that is, on the hexagonal faces of the Brillouin zone, and along the line V in Fig. 4.

It is hardly worth while trying to extract more information from the free-electron model, which will certainly not be correct in detail. It will be a useful guide, however, in the interpretation of the results of the calculation by augmented plane waves, when those results are available.

[9] R. G. Chambers, *The Fermi Surface* (John Wiley & Sons, Inc., New York, 1960), p. 100, includes a good description of this effect, with references.

APPENDIX I

Consider a space group, of order gN, consisting of N primitive translations and a point group of order g. For this group we construct a representation in the following way. Imagine that we have a function $f(\mathbf{r})$ with no special translational or rotational symmetry properties, and construct from it the gN functions

$$u_{\mathbf{k},\alpha}=\sum(\mathbf{R}_n)\exp(-i\mathbf{k}\cdot\mathbf{R}_n)\{\epsilon|\mathbf{R}_n\}\{\alpha|\mathbf{a}\}f(\mathbf{r}), \quad \text{(A1)}$$

where $\{\epsilon|\mathbf{R}_n\}\{\alpha|\mathbf{a}\}$ is one of the operations of the group in Seitz's notation. Here $\mathbf{R}_n$ is a primitive translation, ϵ is the identity, α is a member of the point group, and $\mathbf{a}$ is a nonprimitive translation which may be associated with α. $\mathbf{k}$ is one of the N inequivalent wave vectors in or on the surface of the first Brillouin zone. Associated with a given wave vector $\mathbf{k}$ there are n_s distinct wave vectors, belonging to a star, related by

$$\begin{aligned}\mathbf{k}_i&=\alpha\mathbf{k},\\ \mathbf{k}_i-\mathbf{k}_j&\neq\mathbf{K},\end{aligned} \quad \text{(A2)}$$

where $\mathbf{K}$ is a primitive translation of the reciprocal lattice in $\mathbf{k}$ space, and the index i runs from 1 to n_s. It is not hard to see that the gn_s functions $u_{\mathbf{k}_i,\alpha}$ ($i=1\cdots n_s$; α runs over the point group) form a basis for a reducible representation of the space group.

We now wish to find the number of times the mth irreducible representation of the space group associated with the star s is contained in the reducible representation described above. We use the group-theoretical theorem $\sum(\text{operations})\ \chi^*\chi_m=c_m$ times the number of operators in the group, where χ is the character of the reducible representation, χ_m is the character of the desired irreducible representation, and c_m the desired number. We first find the character of the reducible representation. The only matrices in this representation that have diagonal elements are those corresponding to the primitive translations. If we call $\chi_s(\{\alpha|\mathbf{a}+\mathbf{R}_n\})$ the characters of this representation, we can see that

$$\chi_s(\{\alpha|\mathbf{a}+\mathbf{R}_n\})=\delta_{\alpha,\epsilon}g\sum_{i=1}^{n_s}\exp(i\mathbf{k}_i\cdot\mathbf{R}_n). \quad \text{(A3)}$$

Next we find the character of the irreducible representation. For an irreducible representation of a space

group, the character associated with a translation $\{\epsilon|\mathbf{R}_n\}$ is

$$d_{m,s}\sum_{j=1}^{n_s}\exp(i\mathbf{k}_j\cdot\mathbf{R}_n), \tag{A4}$$

where $d_{m,s}$ is the dimension of the mth irreducible representation of the group of the wave vector $\mathbf{k}$. From Eqs. (A3) and (A4), and the theorem quoted above, the number of times the mth irreducible representation of the space group associated with the star s is contained in the reducible representation is then

$$\begin{aligned}c_{m,s}&=(1/gN)\sum(R_n)\sum_{i,j=1}^{n_s}d_{m,s}g\exp[i(\mathbf{k}_j-\mathbf{k}_i)\cdot\mathbf{R}_n]\\&=(1/gN)\sum_{i,j=1}^{n_s}d_{m,s}gN\delta_{ij}\\&=d_{m,s}n_s.\end{aligned} \tag{A5}$$

We now use the fact that the gn_s basis functions in the reduction of the reducible representation must be made up out of sets of $n_sd_{m,s}$ functions for the various irreducible representations of the space group; the dimensionality of such an irreducible representation equals the product of $d_{m,s}$, the dimensionality of the group of the wave vector, and n_s, the number of wave vectors in the star. We have seen in Eq. (A5) that we have $c_{m,s}$ different sets of basis functions for the mth irreducible representation. We then have that

$$gn_s=\sum(m)c_{m,s}n_sd_{m,s}=\sum(m)(d_{m,s}n_s)^2. \tag{A6}$$

This is what we set out to prove. As a simple corollary, we see that

$$(g/n_s)=\sum(m)(d_{m,s})^2. \tag{A7}$$

Here (g/n_s) is the order of the point group associated with the wave vector $\mathbf{k}$. In words: the sum of the squares of the dimensionalities of the irreducible representations of the group of the wave vector equals the order of the point group of the group of the wave vector.

PHYSICAL REVIEW VOLUME 126, NUMBER 4 MAY 15, 1962

Effects of Spin-Orbit Coupling in Si and Ge*†

L. Liu‡
Department of Physics and Institute for the Study of Metals, University of Chicago, Chicago, Illinois, and Argonne National Laboratory, Argonne, Illinois

(Received December 18, 1961)

A treatment of spin-orbit effects in some semiconductors is given using the effective-mass method and orthogonalized-plane-wave type wave functions. In this formalism, the spin-orbit splitting of valence states in the crystal is expressed directly in terms of either experimental or calculated values of the spin-orbit splitting of the atomic-core states. The calculation yields values in good agreement with experiments for the splitting at $\Gamma_{25'}$ for Si and at both $\Gamma_{25'}$ and $L_{3'}$ for Ge. A demonstration is given of the enhancement of the spin-orbit splitting of valence states in the crystal over the corresponding atomic value.

The shift in the g tensor due to spin-orbit interactions is studied in Si and Ge. Because of crystal selection rules, the usual two-band approximation to the effective-mass sum rule is inadequate for Si and, in particular, the core state must be considered. When all important states are included, the calculations yield values in good agreement with experiment. In the case of Ge, it is found that core states do not contribute appreciably to the g tensor. However, the calculated value for the shift in the transverse component of the g tensor has an opposite sign to the measured one.

A certain matrix element of the deformation potential for Si is also evaluated based on the measured shift in the g value due to strain. The result is compared with other deformation potentials in Si.

I. INTRODUCTION

THE effects of spin-orbit (s-o) coupling on the electronic properties of crystals have been discussed by several authors.[1–6] For semiconductors, these properties are largely determined by the nature of the conduction and valence band edges. In semiconductors where these band edges are of p atomic symmetry and split under the s-o interaction, knowledge of the magnitude of their s-o splittings becomes necessary in any quantitative calculations. Although there have been recently several direct measurements of the valence state s-o splitting for[7] Si and[8] Ge by optical experiments, there is lack of any quantitative estimate in theory. In this work we attempt to estimate the s-o

* A thesis submitted to the Department of Physics, the University of Chicago, in partial fulfillment of the requirements for the Ph.D. degree.

† Based on work performed under the auspices of the U.S. Atomic Energy Commission and supported in part by the Office of Naval Research and the National Science Foundation.

‡ Now at the Department of Physics, Northwestern University, Evanston, Illinois.

[1] R. J. Elliott, Phys. Rev. **96**, 266, 280 (1954).
[2] Y. Yafet, Phys. Rev. **85**, 478 (1952).
[3] L. M. Roth, B. Lax, and S. Zwerdling, Phys. Rev. **114**, 90 (1959).
[4] L. M. Roth, Phys. Rev. **118**, 1534 (1960).
[5] M. H. Cohen and E. I. Blount, Phil. Mag. **5**, 115 (1960).
[6] M. H. Cohen and L. M. Falicov, Phys. Rev. Letters **5**, 544 (1960).
[7] S. Zwerdling, K. J. Button, B. Lax, and L. M. Roth, Phys. Rev. Letters **4**, 173 (1960).
[8] A. H. Kahn, Phys. Rev. **97**, 1647 (1955); M. Cardona and H. S. Sommers, *ibid.* **122**, 1382 (1961); J. Tauc and A. Abraham, *Proceedings of the International Conference on Semiconductor Physics, Prague, 1960* (Czechoslovakian Academy of Sciences, Prague, 1961).